The EMBO Journal vol.14 no.3 pp.409–421, 1995

Suppression of villin expression by antisense RNA impairs brush border assembly in polarized epithelial intestinal cells

Marie-Alyette Costa de Beauregard, Eric Pringault, Sylvie Robine and Daniel Louvard[1]

Institut Pasteur, Département de Biologie Moléculaire, 25 rue du Dr Roux, 75724 Paris Cedex 15, France

[1]Corresponding author

M.-A.Costa de Beauregard and E.Pringault contributed equally to this work

Communicated by D.Louvard

We have used an antisense RNA strategy to investigate the role of the actin-associated protein, villin, in the brush-border morphogenesis of human intestinal CaCO2 cells. Stable expression of a cDNA encoding antisense villin RNA resulted in the permanent down-regulation of the endogenous villin message and dramatically affected brush-border assembly. Ultrastructural and immunolocalization studies revealed that epithelial cell polarity was largely maintained. However, in contrast to brush-border markers such as dipeptidyl-peptidase IV, the apical localization of sucrase-isomaltase was specifically impaired. Retransfection of the villin antisense-expressing cell line with a cDNA encoding a partial sense villin RNA restored both brush-border assembly and sucrase-isomaltase apical expression. The suggestion that brush-border morphogenesis may be important for the trafficking of certain proteins is discussed.

Key words: antisense RNA/cytoskeleton/intestinal cells/sucrase-isomaltase/villin

Introduction

The establishment and maintenance of membrane and cytoskeletal protein asymmetry is a necessary prerequisite for polarized enterocyte functions such as the digestion and vectorial transport of nutrients. For example, the apical surface of intestinal cells is greatly amplified by the formation of an ordered array of microvilli, the brush border. The characterization of the protein components which serve to organize this specialized domain has been the focus of many studies. The brush-border membrane is supported by a bundle of actin microfilaments containing several actin binding proteins, including two F-actin cross-linkers, villin and fimbrin, and a protein complex composed of brush-border myosin I associated with three to four molecules of calmodulin, which connect the F-actin bundles to the plasma membrane (Bretscher, 1991; Arpin and Friederich, 1992).

Experimental evidence *in vitro* suggests that brush-border morphogenesis is driven simply by the auto-assembly of individual cytoskeleton components (Coluccio and Bretscher, 1989). Developmental studies indicate that brush-border assembly is a multistep process where the individual cytoskeletal proteins are recruited in a stepwise fashion to the luminal surface of intestinal cells, corresponding to the progressive elaboration of microvillar structures (Heintzelman and Mooseker, 1992; Mamajiwalla *et al.*, 1992). This 'stepwise' process has also been described *in vitro* (Peterson and Mooseker, 1993; Peterson *et al.*, 1993). In this study we have assumed that the morphogenesis of a brush border could be interrupted at different steps by inhibiting the expression of one of its major components. The suppression of an individual brush-border component would alter the brush border in such a way as to lead to a better understanding of the particular component function. Moreover, it would enable us to identify the functions which are maintained or lost when the cytoskeleton is partially or completely disorganized.

To help us to achieve this goal, we chose to suppress villin expression in cultured intestinal CaCO2 cells which manifest a well-developed brush border. There are several arguments which favor a major role of villin in brush-border cytoskeleton assembly. Unlike most actin binding proteins, including fimbrin, villin expression is tissue specific (Robine *et al.*, 1985; Pringault *et al.*, 1986), mainly restricted to cells which display a well-developed brush border (intestinal epithelial cells, renal proximal tubular cells and testis efferens duct cells). Moreover, during embryonic development, while most brush-border proteins are diffusively distributed in the cytoplasm, villin is the first to be apically localized (Shibayama *et al.*, 1987). In the course of enterocytic migration and differentiation from the crypt towards the villus, the amount of villin increases dramatically and is concurrent with the appearance of brush-border microvilli (Robine *et al.*, 1985; Boller *et al.*, 1988). It has been proposed, therefore, that villin plays a major role in the initiation of brush-border assembly. This hypothesis has been tested by transfecting the villin cDNA into non-polarized CV1 cells which do not normally express the protein. High levels of villin expression were sufficient to induce the appearance of numerous, long and rigid microvillar structures (Friederich *et al.*, 1989, 1992).

We decided to suppress villin expression using antisense RNA technology which has greatly facilitated the understanding of protein function in the context of its normal cellular environment. The molecular tools required were developed previously in our laboratory (Arpin *et al.*, 1988; Pringault *et al.*, 1991; Robine *et al.*, 1993). The antisense RNA approach was first used to suppress non-muscle actin gene expression in a culture cell line (Izant and Weintraub, 1985). More recently it has been used to suppress the expression of a number of other cytoskeletal proteins in cultured cells, such as myosin heavy chain

(Knecht and Loomis, 1987), myosin light chain (Pollenz *et al.*, 1992), glial fibrillary acidic protein (Weinstein *et al.*, 1991) and vinculin (Rodriguez Fernandez *et al.*, 1993). This approach has also been applied to protein 4.1 in the *Xenopus* embryo (Giebelhaus *et al.*, 1988), and myelin basic protein in transgenic mice (Katsuki *et al.*, 1988).

In our study we show that a sustained down-regulation of endogenous villin expression in CaCO2 cells dramatically alters brush-border assembly. It is interesting to note that while epithelial polarity appeared unaffected as determined by a number of criteria, the brush-border enzyme sucrase-isomaltase (SI) was no longer observed at the apical membrane but instead was localized intracellularly. Super-transfection of the antisense-expressing cells with a construct coding for a partial sense villin RNA restored the parental CaCO2 phenotype, strongly supporting the notion that villin is necessary for both the cytoskeletal and membrane protein organization of a functional brush border.

Results

Stable expression of villin antisense RNA in CaCO2 clone 1 cells dramatically decreases villin expression

We have shown previously that the half-life of villin is >72 h (Dudouet *et al.*, 1987; Boller *et al.*, 1988). Since transient expression of antisense RNA might not reduce the steady-state level of a protein with such a long half-life, we decided to generate stable transfectants in the CaCO2 intestinal cell line (Fogh and Trempe, 1975) using the pCB6 eukaryotic expression vector.

It is widely held that the original CaCO2 cell line displays great phenotypic heterogeneity in cell culture. However, it has been shown previously that CaCO2 subclones displaying morphological homogeneity (e.g. well organized brush-border expression and strong apical villin expression) and functional homogeneity (e.g. brush-border hydrolase expression) can be obtained, although the level of SI expression could vary from one cell to another (Peterson and Mooseker, 1992). To be certain that the morphogenetic effects of antisense villin expression are due to the antisense itself and not to the heterogeneity of the parental cell line, we have isolated by a limiting dilution procedure subclones of CaCO2 cells which display a high degree of homogeneity. One clone referred to as CaCO2 clone 1 displayed the features required for the present studies, characterized by a well-organized brush border and high, homogeneous levels of villin expression (Figure 1).

A 1274 bp 5′ fragment spanning the ATG translation initiator of the villin cDNA was inserted in the reverse orientation in the pCB6 expression vector downstream from the cytomegalovirus (CMV) promoter (Figure 2A). The resulting construct pCB6 AS 4.8, which expresses villin antisense RNA, was used to transfect the CaCO2 clone 1.

Subclones resistant to G418 were isolated. To check that transfection and selection with G418 did not perturb the CaCO2 clone 1 phenotype, we cotransfected CaCO2 clone 1 cells with one construct containing the Neo^R gene together with a second construct containing the firefly luciferase gene as an exogenous reporter gene. After selection with G418, these double-transfected cells displayed the same phenotype as CaCO2 clone 1 parental cells (see Materials and methods).

In villin antisense clones the presence of the villin antisense construct was monitored by PCR amplification with genomic DNA. The choice of the two primers allowed us to discriminate between amplification of the transgene and amplification of the endogenous villin gene (see Materials and methods). Western blot analysis was performed on 14 independent Neo^R cell clones transfected with pCB6 AS 4.8. Actin immunodetection, used as an internal control, showed that the steady-state level of this protein was not affected. We found that the level of endogenous villin varied dramatically between individual clones. Although total suppression of villin was never achieved, we selected two clones (CaCO2 AS 4.8/21 and CaCO2 AS 4.8/34) where the level of villin expression was reduced significantly (Figure 2B). CaCO2 AS 4.8/34 (lane 3) has the lowest residual level of villin expression and CaCO2 AS 4.8/21 (lane 2) displays an intermediate level when compared with wild-type CaCO2 cells and CaCO2 AS 4.8/34. Northern blot analysis revealed that these clones displayed only a slight decrease in the level of villin mRNA compared with that observed in the parental CaCO2 clone 1 (data not shown). This indicated that while the endogenous villin gene was transcribed at a normal rate, its translation into protein product was impaired as has been described in other antisense experiments (Kim and Wold, 1985). However, the villin antisense RNA could not be detected by Northern blot analysis as reported in previous studies (Colman, 1990). The low level of antisense RNA has been investigated using a sensitive assay. For this purpose we performed RNase protection experiments using a sense radiolabeled RNA probe, with either CV1 cells transiently transfected with the antisense RNA-encoding plasmid pCB6 AS 4.8 (referred to as CV1 AS 4.8 cells) or the CaCO2 AS 4.8/34 clone. Employing this procedure we observed a strong signal in CV1 AS 4.8 cells and a weaker signal in CaCO2 AS 4.8/34 cells (data not shown). We concluded that villin antisense RNA was efficiently transcribed from the pCB6 AS 4.8 construct both in CV1 AS 4.8 cells and in our clone CaCO2 AS 4.8/34. In contrast to CaCO2 AS 4.8/34 cells, CV1 AS 4.8 cells did not produce the endogenous villin mRNA. Thus, competition between the RNA probe and villin endogenous mRNA might account for the lower signal observed in CaCO2 AS 4.8/34 cells.

Expression of villin antisense RNA results in the complete disorganization of brush-border microvilli

Scanning electron microscopy was used to visualize the apical cell surfaces of parental CaCO2 cells and isolated mutants (Figure 3). While the apical surfaces of CaCO2 clone 1 cells were covered with densely packed microvilli clustered by their tips (a feature reported previously by others for these human intestinal cells; Figure 3a), the apical surfaces of CaCO2 AS 4.8/34 cells which expressed the lowest level of villin displayed much fewer microvilli that were both sparsely distributed and short in nature (Figure 3c). The CaCO2 AS 4.8/21 clone, which produced

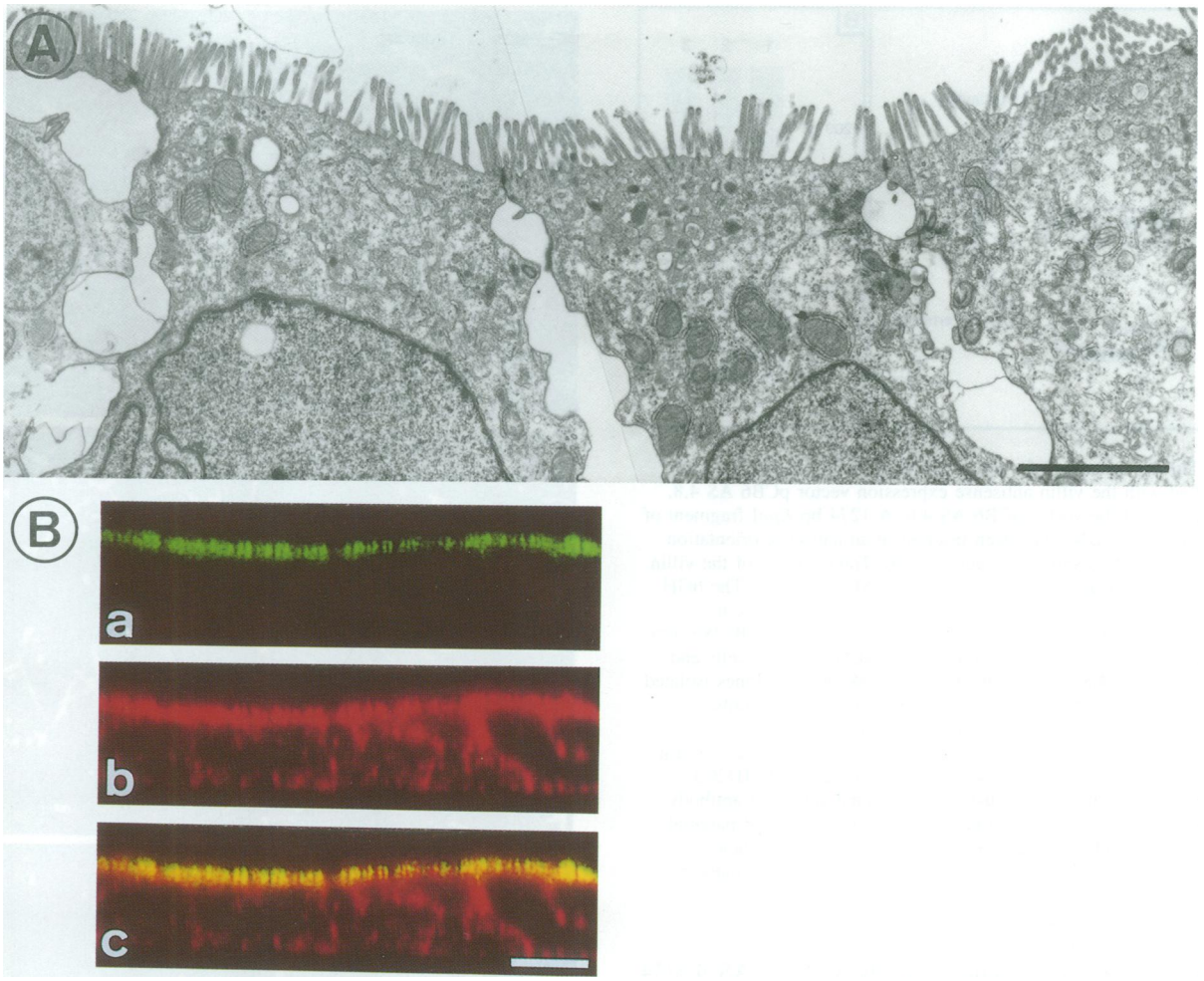

Fig. 1. The apical domain of CaCO2 clone 1 cells is uniformly organized. (**A**) CaCO2 clone 1 cells grown on plastic dishes were analyzed 10 days after confluency by transmission electron microscopy. Transverse section of the cell monolayer. CaCO2 clone 1 cells are well polarized and display a continuous brush border at their apical surfaces, as well as well-developed junctional complexes. Bar corresponds to 0.4 μm. (**B**) CaCO2 clone 1 confluent cells were analyzed by CLSM after double-immunolabeling with a monoclonal anti-villin antibody and rhodamine-coupled phalloidin. Vertical ($x-z$) optical sections. (**a**) Villin labeling is intense at the apex of the cells. (**b**) F-actin staining is concentrated at the apical faces, and under the basolateral membranes as a cortical thin layer of F-actin microfilaments. (**c**) Superposition of images (a) and (b) illustrates the colocalization of villin and F-actin at the apices of the cells. Bar corresponds to 10 μm.

villin at a level intermediate to the parental CaCO2 clone 1, and the CaCO2 AS 4.8/34 similarly displayed an intermediate brush-border phenotype. Indeed, the CaCO2 AS 4.8/21 clone displayed a less perturbed phenotype than the CaCO2 AS 4.8/34 clone. Its apical surface exhibited longer microvilli than the CaCO2 AS 4.8/34 clone, although dispersed and no longer in close contact at their tips (Figure 3b), like the CaCO2 clone 1.

Transmission electron microscopy performed on 50 nm sections confirmed the disappearance of highly ordered microvilli at the apex of the CaCO2 AS 4.8/34 cells (Figure 4). Moreover, in contrast to the microvilli observed in the parental CaCO2 cell line (clone 1; Figure 4a), the few remaining microvilli observed in CaCO2 AS 4.8/34 cells (Figure 4c) appeared limp. While the bundles of actin filaments were well visualized in the microvillar core of the parental CaCO2 clone (Figure 4a), bundles were not observed in the rudimentary microvilli of the CaCO2 AS 4.8/34 clone (Figure 4c). It is interesting to note that the electron dense plaque, found at the tip of the microvillus and believed to be the attachment site for F-actin bundles, was not observed in microvilli of CaCO2 AS 4.8/34 cells. In the CaCO2 AS 4.8/21 clone a less perturbated phenotype was confirmed; while apical microvilli were fewer, bundles of actin filaments could be observed in their core. These microvilli resembled the parental CaCO2 brush-border microvilli, but were shorter and much less abundant.

Morphometric analysis performed on 100 cells indicated that the density of the apical microvilli in CaCO2 clone 1 cells was 3.5 times greater than in CaCO2 AS 4.8/34 cells. Moreover, the mean value of their length was measured to be 1.33 μm in CaCO2 clone 1 cells and 0.47 μm in CaCO2 AS 4.8/34 cells, which corresponds to a diminution of 65% of their length.

These data led us to conclude that the extent of apical microvilli organization in CaCO2 cells is linked to the steady-state level of villin expression. When villin expression is almost abolished, organized microvilli cannot develop; when villin production is only partially reduced, microvilli can begin to develop into an organized brush border.

For further characterization of the consequences of antisense villin RNA expression on CaCO2 clone 1 cells,

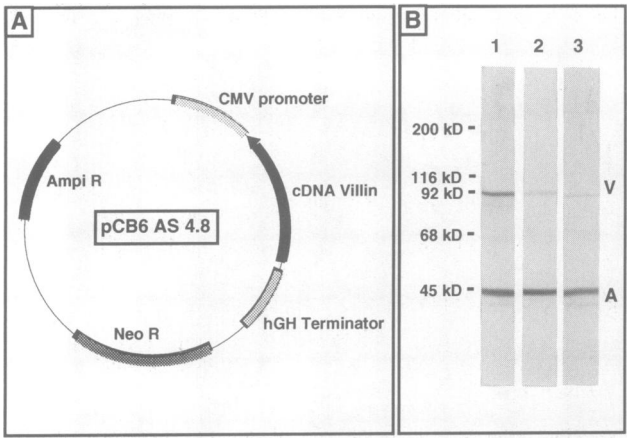

Fig. 2. Down-regulation of villin expression in CaCO2 clone 1 cells transfected with the villin antisense expression vector pCB6 AS 4.8. (**A**) Structure of the vector pCB6 AS 4.8. A 1274 bp *KpnI* fragment of the human villin cDNA has been inserted in an antisense orientation into the eukaryotic expression vector pCB6. Transcription of the villin antisense cDNA fragment is driven by the CMV promoter. The hGH terminator provides the RNA processing signal. The neomycin acetyltransferase gene (Neo^R) confers resistance to G418. (**B**) Western blot analysis of cell extracts from parental CaCO2 clone 1 cells and from CaCO2 AS 4.8/21 and CaCO2 AS 4.8/34, two subclones isolated after transfection with the pCB6 AS 4.8 vector. Equal amounts (100 µg) of total cell protein extracts were separated by electrophoresis and blotted onto nitrocellulose. The presence of villin (V) was detected with the monoclonal anti-villin antibody ID2C3. Immunodetection of actin (A) using a polyclonal anti-actin antibody was performed as an internal control. Lane 1, untransfected parental CaCO2 clone 1 cells; lane 2, CaCO2 AS 4.8/21 subclone; lane 3, CaCO2 AS 4.8/34 subclone. Positions of molecular weight markers are indicated.

we chose to focus our studies on the CaCO2 AS 4.8/34 cells which offered the most altered phenotype.

Distribution of actin filaments is strongly modified in CaCO2 AS 4.8/34 cells

The distribution of F-actin was compared between CaCO2 AS 4.8/34 cells and the parental clone using fluorescein-conjugated phalloidin. In the parental cells, F-actin staining was essentially localized to the apex of the cells within the brush border (Figure 5a). In the basal region of the cells, stress fibers were poorly represented in confluent CaCO2 cells, as is usual for cells that have reached confluency (Figure 5b). Instead, F-actin staining was localized just under the plasma membrane and concentrated in adhesion foci. In striking contrast, minimal F-actin staining was detected at the apex of the CaCO2 AS 4.8/34 subclone, in agreement with the disappearance of F-actin bundles observed by transmission electron microscopy (Figure 5c). Instead, F-actin staining was seen primarily along stress fibers in the basal region of the confluent CaCO2 AS 4.8/34 cells (Figure 5d). It is worth mentioning that the total amount of G/F-actin was not affected in the antisense-expressing cells, as demonstrated by Western blot analysis (Figure 2B).

CaCO2 AS 4.8/34 cells maintain a polarized epithelial phenotype despite the absence of a well-developed brush border

The ultrastructural studies reported above suggested that despite the absence of a morphologically distinct brush

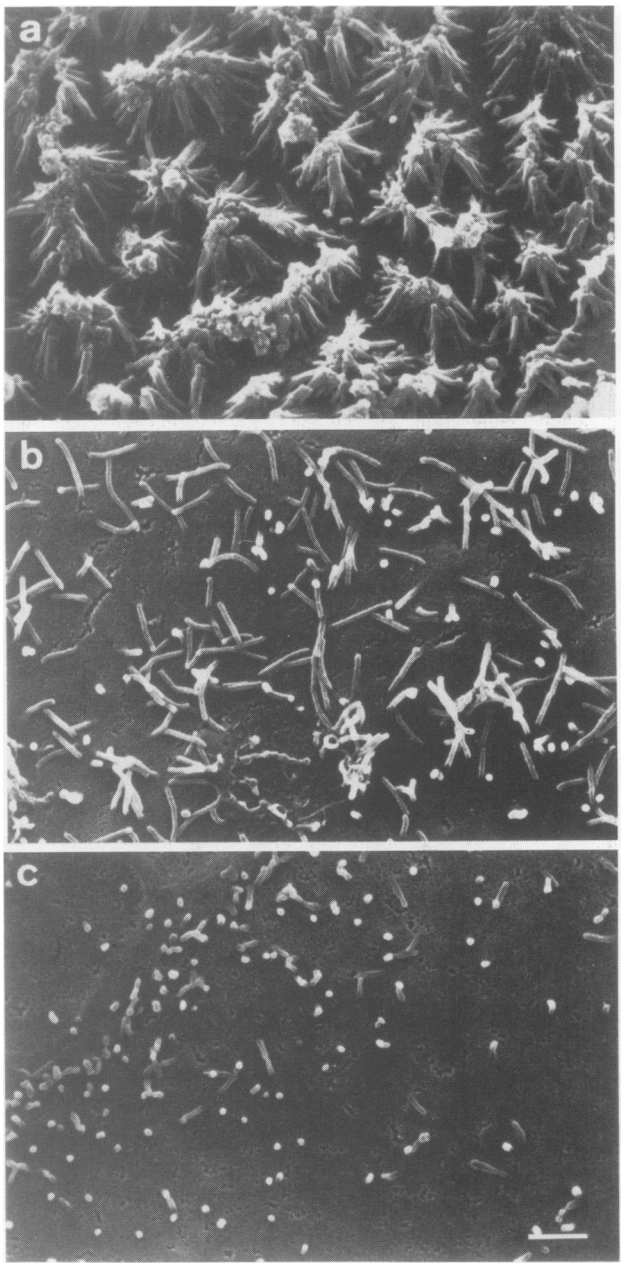

Fig. 3. Scanning electron microscopy reveals modifications of the organization of the apical cell surface in the antisense villin RNA CaCO2 subclones. Parental CaCO2 clone 1 cells, CaCO2 AS 4.8/21 subclone and the CaCO2 AS 4.8/34 subclone were analyzed 10 days after confluency by scanning electron microscopy. (**a**) Apical cell surface of untransfected CaCO2 clone 1 cells (control cells). The apical cell surface is covered by dense, long, rigid and packed microvilli characteristic of a well-differentiated brush-border structure. (**b**) Apical cell surface of CaCO2 AS 4.8/21 subclone transfected with antisense villin cDNA. The cell surface is supported by sparse microvilli which appear rigid but shorter than in CaCO2 parental cells. (**c**) Apical cell surface of CaCO2 AS 4.8/34 subclone transfected with antisense villin cDNA. In contrast to control cells, the apical cell surface is nearly devoid of microvilli. The few remaining microvilli appear to be short, sparse and limp. Bar corresponds to 1 µm.

border, CaCO2 AS 4.8/34 cells appeared to maintain the gross organizational characteristic of polarized epithelial cells. For example, these cells were able to grow in

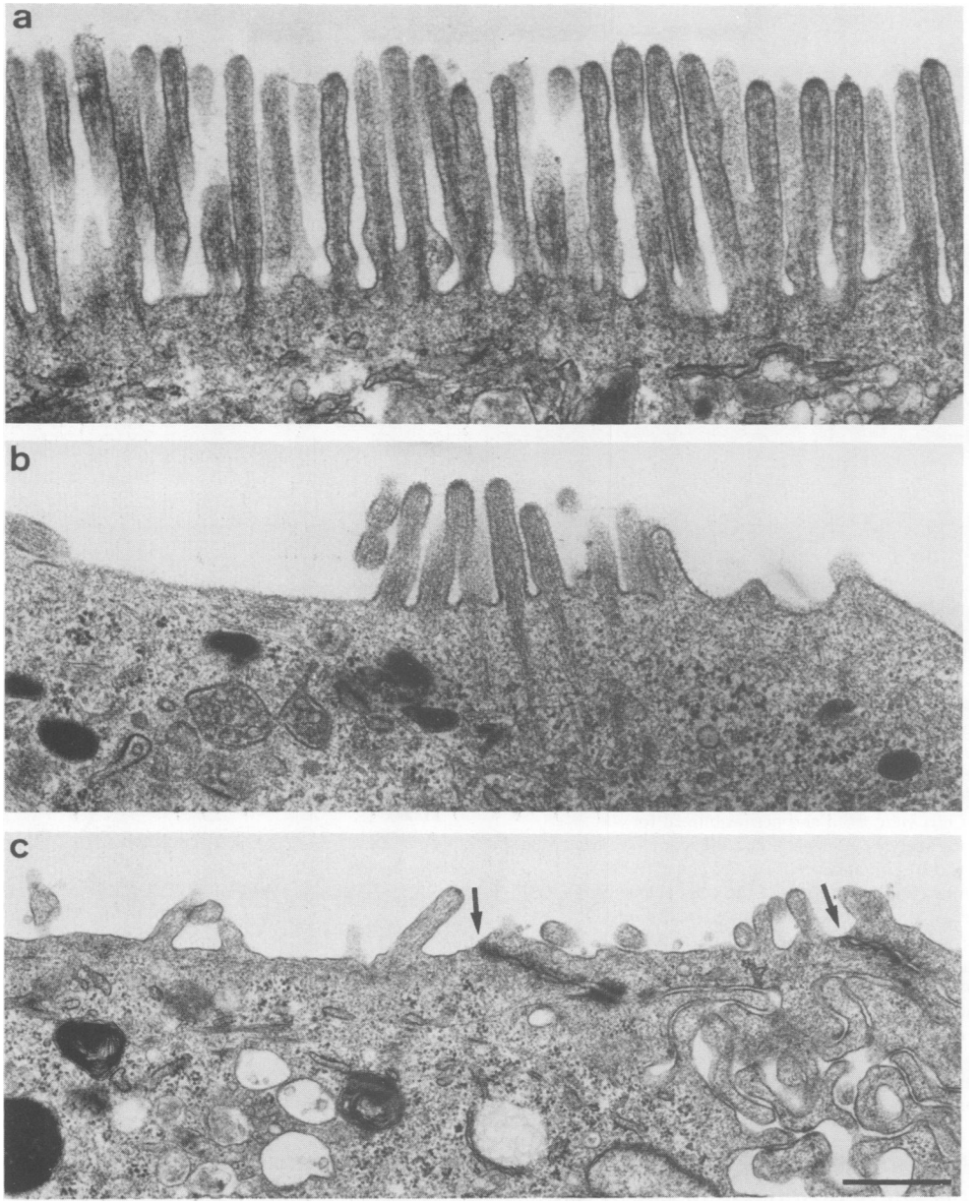

Fig. 4. Transmission electron microscopy shows the absence of a well-developed brush border in the two subclones and the lack of ordered F-actin bundles in the microvillar core of CaCO2 AS 4.8/34 cells. Parental CaCO2 clone 1 cells, and both the CaCO2 AS 4.8/21 and CaCO2 AS 4.8/34 subclones, were analyzed 10 days after confluency by transmission electron microscopy. (**a**) Transverse sections of the apical domain of untransfected CaCO2 clone 1 cells. Dense and ordered microvilli demonstrate an organized brush border. Dense bundles of microfilaments are clearly visible in the core of the microvillus. These bundles extend into the underlying cytoplasm. (**b**) Transverse sections of the apical domain of the CaCO2 AS 4.8/21 subclone transfected with villin antisense cDNA. Microvilli are organized as in CaCO2 parental cells, but they appear shorter and cover only a small part of the cell surface. (**c**) Transverse sections of the apical domain of the CaCO2 AS 4.8/34 subclone transfected with villin antisense cDNA. In these cells, which express a very low level of villin, the apical microvilli are dispersed, short and disorganized. Microfilament bundles are not observed in the cores of the 'stunted' microvilli. A typical junctional complex is illustrated, displaying a tight junction, an adherens junction and a desmosome (arrows). Bar corresponds to 0.5 μm.

monolayers, as observed at a low magnification (data not shown), and displayed typical junctional complexes (Figure 4c).

To investigate further the membrane and cytoskeletal polarity in these CaCO2 AS 4.8/34 cells, confocal laser scanning microscopic (CLSM) immunocytochemical analysis was performed on the tight junction protein ZO1 (Anderson *et al.*, 1989) and the basolateral marker 120 kDa glycoprotein (Eilers *et al.*, 1989). An optical section in the horizontal ($x-y$) plane showed that the tight junction protein, ZO1, clearly delineates cell–cell contacts (Figure 6a). An optical section perpendicular to the plane of the monolayer ($x-z$) showed that this staining was restricted exclusively to focal spots between the cells at their apices (Figure 6b). Immunolabeling with an antibody specific for the gp120 gave a typical basolateral pattern (Figure 6c; Louvard, 1980). Interestingly, the optical section in an $x-z$ axis (Figure 6d) revealed that this protein was more abundant near the junctional complexes of the lateral membranes. Localizations of these two markers in the parental CaCO2 clone 1 cells were identical to those observed in the antisense-expressing cells (data not shown).

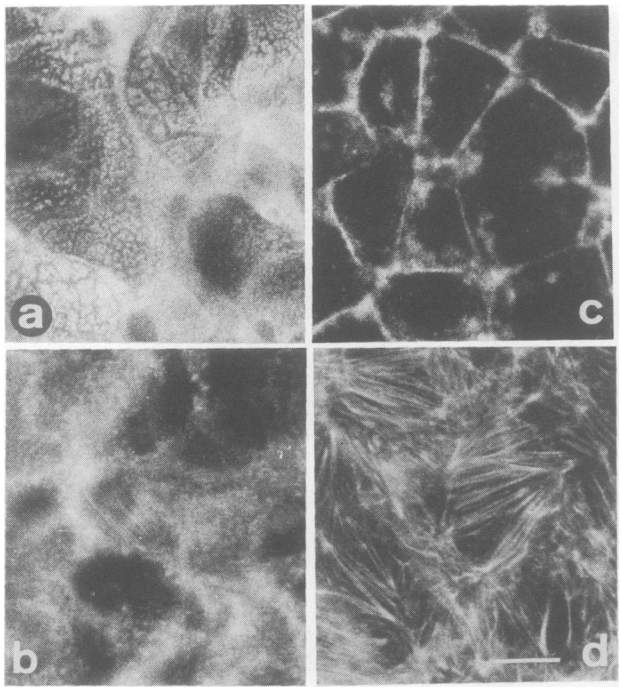

Fig. 5. Suppression of villin synthesis in the CaCO2 AS 4.8/34 subclone correlates with the absence of apical F-actin bundles and the persistence of stress fibers after confluency. F-actin was stained with rhodamine-coupled phalloidin in both untransfected CaCO2 clone 1 cells and the CaCO2 AS 4.8/34 subclone transfected with the villin antisense cDNA. Cells were fixed and permeabilized for immunofluorescence analysis 10 days after confluency (see Materials and methods). (**a** and **b**) Untransfected CaCO2 clone 1 cells. (a) Intense F-actin labeling at the apex of the cells characterizes a fully developed brush border. (b) At the bottom of the cells, F-actin labeling surrounds the plasma membrane and is concentrated in adhesion foci. Very few stress fibers are observed. This labeling can be compared with the vertical ($x-z$) optical section by CLSM analysis in Figure 1. (**c** and **d**) CaCO2 AS 4.8/34 subclone transfected with villin antisense cDNA. (c) F-actin labeling is very poor at the apex of the cells, and instead is concentrated mainly beneath the lateral membrane. (d) Numerous stress fibers are clearly visualized at the bottom of the cells. Bar corresponds to 20 μm.

Unlike other brush-border hydrolases, SI is not detected at the apical membrane of CaCO2 AS 4.8/34 cells

We wished to determine the extent to which apical membrane proteins were properly localized in CaCO2 AS 4.8/34 cells, despite the absence of a brush border. Immunocytochemical studies were performed on three brush-border hydrolases: dipeptidyl-peptidase IV (DPP IV), neutral amino-peptidase (nAP) and neutral endo-peptidase (nEP). Specific antibodies were applied to fixed and non-permeabilized monolayers, thus allowing us to detect hydrolases actually present within the apical cell membrane. CLSM analysis (optical sections in the $x-y$ axis) showed that DPP IV was detected in the apical membrane of CaCO2 AS 4.8/34 cells; however, the labeling appeared less intense than on the parental CaCO2 cells (Figure 7a and b). This decrease in fluorescence intensity might correlate with the reduction of apical cell surface area observed in the mutant cells (Figure 3c). Similar results were obtained using anti-nAP and anti-nEP antibodies (data not shown). These results confirm the epithelial polarity of the CaCO2 AS 4.8/34 subclone and show that the delivery and residence of these apical markers is not affected by the absence of a well-differentiated brush border.

However, it is interesting to note that not all brush-border hydrolases are properly localized in this mutant clone. SI is a hydrolase which, in contrast to DPP IV, nAP and nEP, is uniquely inserted in the brush-border membrane of epithelial cells of the small intestine. In non-permeabilized parental CaCO2 cells, SI was readily detected and displayed the characteristic pattern observed for apical markers of fully differentiated brush-border membranes (Figure 7c). However, in non-permeabilized CaCO2 AS 4.8/34 cells, no surface labeling of SI could be detected (Figure 7d). This is not because the CaCO2 AS 4.8/34 clone does not express the protein, as SI labeling performed after permeabilization revealed a significant amount of diffuse vesicular staining throughout the cytoplasm (Figure 7f). No such intracellular staining is seen in parental CaCO2 clone (Figure 7e).

Therefore, while CaCO2 AS 4.8/34 cells continue to express SI as a marker of enterocytic differentiation, this enzyme, in contrast to DPP IV, nAP and nEP, does not accumulate in the apical plasma membrane. We suggest that some apical proteins, such as SI, may require the brush-border structure to be properly localized.

Brush-border assembly can be restored in CaCO2 AS 4.8/34 cells upon overexpression of sense villin RNA

A 975 bp 5′ fragment of the villin cDNA was inserted in the pMT/EP expression vector, downstream from the metallothionein (MT) promoter (Figure 8A). The resulting construct, pMT/VIL3, encodes a partial sense villin RNA which is complementary to the antisense villin RNA (see Materials and methods). This sense RNA, overexpressed in CaCO2 AS 4.8/34 cells, would be able to titrate antisense villin RNA. By inhibiting villin antisense hybridization to the endogenous villin messages, we aimed to restore the parental CaCO2 phenotype in these cells after transfection with the pMT/VIL3 construct. The presence of the hygromycin B resistance gene on this vector allowed for the selection of stable double transfectants. Transfection of a partial villin sense RNA isolated from the full-length villin cDNA was chosen to show that restoration of the wild-type brush-border phenotype was due to expression from the endogenous villin gene rather than from the newly transfected pMT/VIL3 construct encoding partial sense villin RNA.

Double resistant clone CaCO2/34/pMT was pooled and cultured in the presence of 1 mM Zn^{2+} to activate the MT promoter. We screened for phenotypic revertants by the immunolocalization of F-actin, villin and SI. Dense apical punctate F-actin labeling was observed at the apical surfaces of large areas of the CaCO2/34/pMT cell monolayer, indicating that F-actin bundles were once again being organized to form a brush border (Figure 8B). As expected, villin expression was recovered in these areas, colocalizing with the apical F-actin labeling (Figure 8C). Furthermore, we detected a large number of cell islands able to express SI at the apical surface membrane. The SI immunofluorescent pattern was identical to that observed in parental cells which exhibit a well-organized brush border (Figure 8D, see also Figure 7c for comparison).

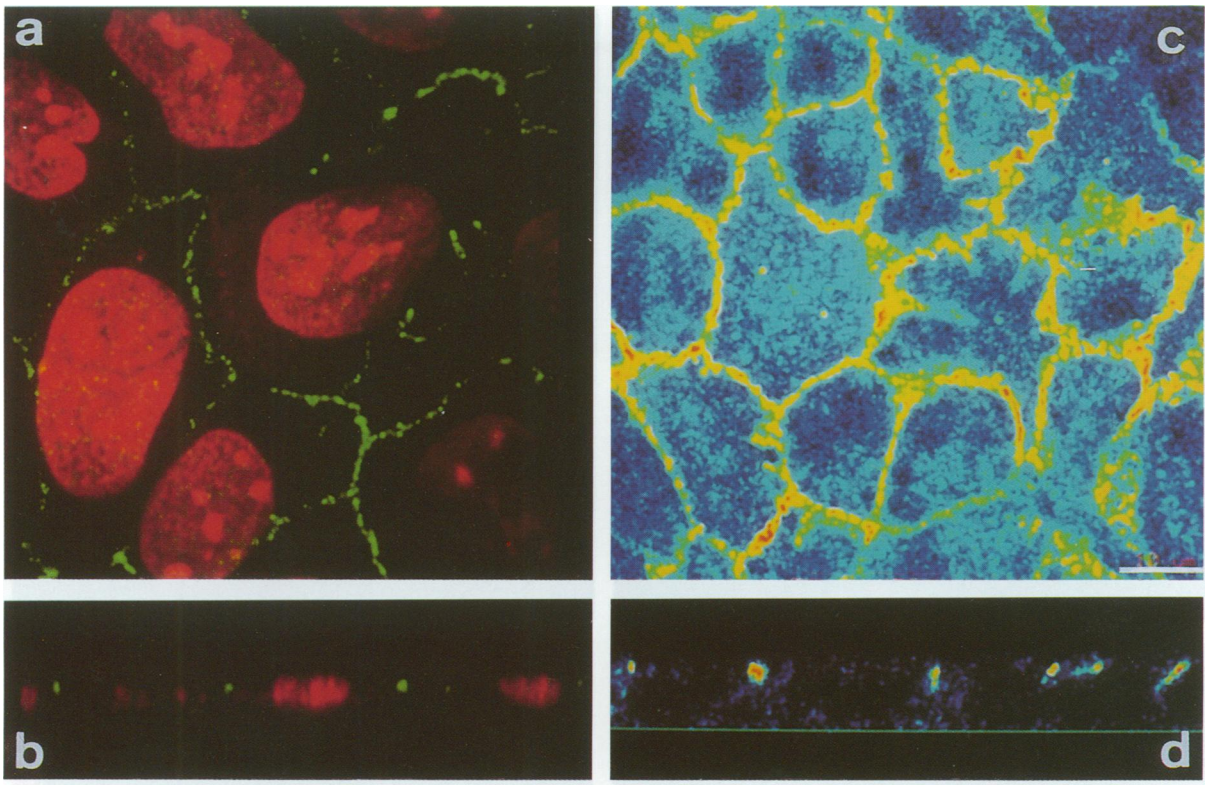

Fig. 6. Antisense villin-expressing cells display a polarized epithelial phenotype. CaCO2 AS 4.8/34 confluent cells were analyzed by CLSM after immunolabeling with antibodies specific for markers of epithelial polarity. (**a** and **b**) CLSM analysis of the tight junction protein ZO1 using a polyclonal anti-ZO1 antibody. The nuclei were visualized by labeling with propidium iodine. (a) Horizontal ($x-y$) optical section. ZO1 labeling is detected along the circumference of the lateral membranes, delineating a ring of cell−cell contacts. (b) Vertical ($x-z$) optical section. ZO1 labeling is restricted to the focal spots between the cells. (**c** and **d**) CLSM analysis of the basolateral gp120 using a monoclonal anti-gp120 antibody. (c) Horizontal ($x-y$) optical section. Labeling of gp120 is restricted to the basolateral membranes. (d) Vertical ($x-z$) optical section. The gp120 is clearly detected at the basolateral membrane and is concentrated near the junctional complexes. Bar corresponds to 10 μm.

Discussion

Villin function is essential and not redundant for brush-border morphogenesis

The biogenesis of the highly ordered bundles of microfilaments present within microvilli may be largely directed by the principles of a self-assembly process of structural proteins, as described for the assembly of bacteriophages, viruses and some large macromolecular complexes. Polarized bundles of actin filaments can be generated in a test tube, provided that only the four major proteins of the microvillus core (actin, fimbrin, villin and brush-border myosin I) are mixed together under appropriate conditions (Coluccio and Bretscher, 1989). Moreover, the stoichiometry of the components found in isolated brush borders appears to be conserved, as lateral brush-border myosin I−calmodulin cross-bridges can be seen forming a regular helix with a pitch of 36 nm. Thus, the spatial organization of these proteins is not dependent upon the participation of specific membrane attachment sites, but rather is determined by the intrinsic properties of the brush-border cytoskeletal components themselves. These intrinsic properties are likely to be the focus of regulation in differentiating intestinal cells. During development in both mammalian and avian intestines, the structural proteins of intestinal microvilli are synthesized very early and accumulate in the cytoplasm, before being recruited from the cytosol to the cell cortex according to a hierarchy of assembly events that involves first villin, followed by fimbrin and then brush-border myosin I (Shibayama *et al.*, 1987; Ezzel *et al.*, 1989). The observed changes in the subcellular distribution of these components correspond to a reorganization of the cortical cytoskeleton and the progressive elaboration of microvilli, which appear to develop from irregular structures containing a loose mesh of microfilaments, into a highly ordered array of polarized actin bundles packed into a hexagonal pattern.

In addition to the changes in the subcellular distribution of the actin binding proteins, an increase in the production of each protein is required. It is well known that self-assembly processes are triggered only when a critical concentration is reached. Complete data are not yet available for three of the major microvillus proteins. However, in the case of villin, immunocytochemical and *in situ* hybridization studies *in vivo*, as well as *in vitro* experiments, support the view that a large cytoplasmic pool of villin is necessary for its morphogenetic activity (Robine *et al.*, 1985; Boller *et al.*, 1988; Friederich *et al.*, 1989; Landry *et al.*, 1994). *In vivo*, the accumulation of high levels of villin transcripts in immature enterocytes correlated with the major morphogenetic changes of the epithelial cells. *In vitro*, the plasma membrane of fibroblasts transfected with the villin cDNA is dramatically remodeled due to the overexpression of villin. In our study we observed that when the level of villin expression was very low in polarized intestinal cells, brush-border microvilli cannot assemble; when this level was increased, the process of brush-border assembly could be initiated.

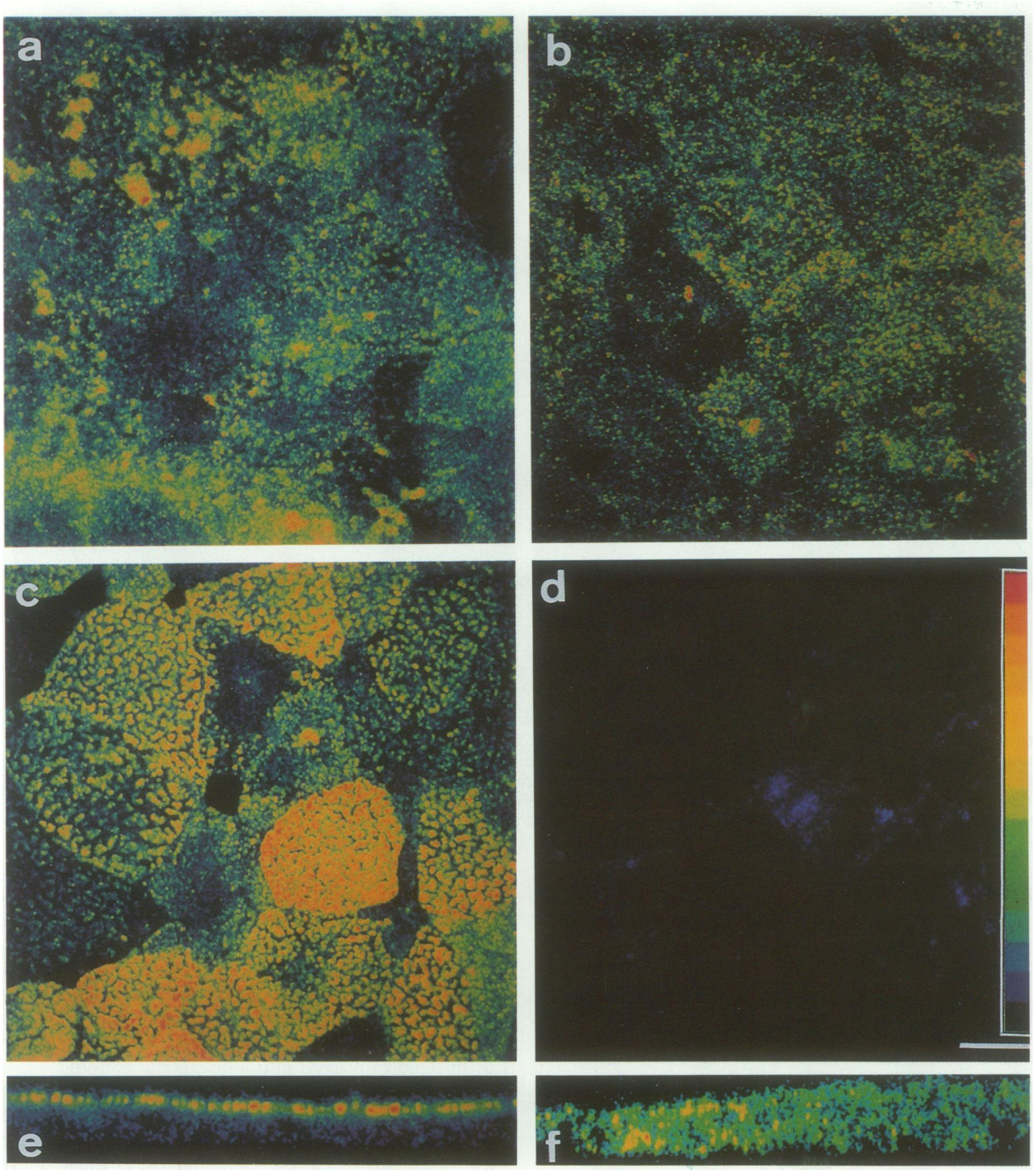

Fig. 7. Insertion of SI into the apical membrane appears to be selectively impaired in antisense villin-expressing cells. Untransfected CaCO2 clone 1 cells and villin antisense transfected CaCO2 AS 4.8/34 cells were analyzed by CLSM. Immunolabeling with antibodies specific for SI or DPP IV was performed 14 days after confluency. The fluorescence intensity is shown by the color scale indicated to the lower right. Red/orange correspond to the highest level of fluorescence intensity, while blue/black correspond to the lowest. (**a**, **c** and **e**) Untransfected CaCO2 clone 1 cells. (**b**, **d** and **f**) CaCO2 AS 4.8/34 subclone transfected with the antisense villin cDNA. (a and b) CLSM analysis (horizontal $x-y$ optical sections) of DPP IV labeling on non-permeabilized cells using a monoclonal anti-DPP IV antibody. Apical staining is detected in both cell lines, although less abundant in CaCO2 AS 4.8/34 cells. (c–f) CLSM analysis of SI immunolabeling using a polyclonal anti-SI antibody. (c) Horizontal ($x-y$) optical section of non-permeabilized CaCO2 clone 1 cells. Note that SI staining is intense, homogeneous and characteristic of a well-differentiated brush border. (d) Horizontal ($x-y$) optical section of non-permeabilized CaCO2 AS 4.8/34 cells. No SI staining is observed. (e) Vertical ($x-z$) optical section of permeabilized CaCO2 clone 1 cells. The SI labeling is largely incorporated within the apical membrane, although faint labeling of biosynthetic compartments can be detected. (f) Vertical ($x-z$) optical section on permeabilized CaCO2 AS 4.8/34 cells. SI labeling is almost exclusively detected in the cytosol. The punctate nature of this staining pattern is perhaps suggestive of vesicular structures. Bar corresponds to 10 μm.

However, sparse clusters of well-ordered microvilli were only seen when the villin level was reduced. The morphogenesis of the apical pole of intestinal cells might be regarded as an assembly line on which a critical concentration of each component is introduced under tight spatio-temporal control.

We chose to explore the role of villin in a cell type which displays a highly developed brush border, the

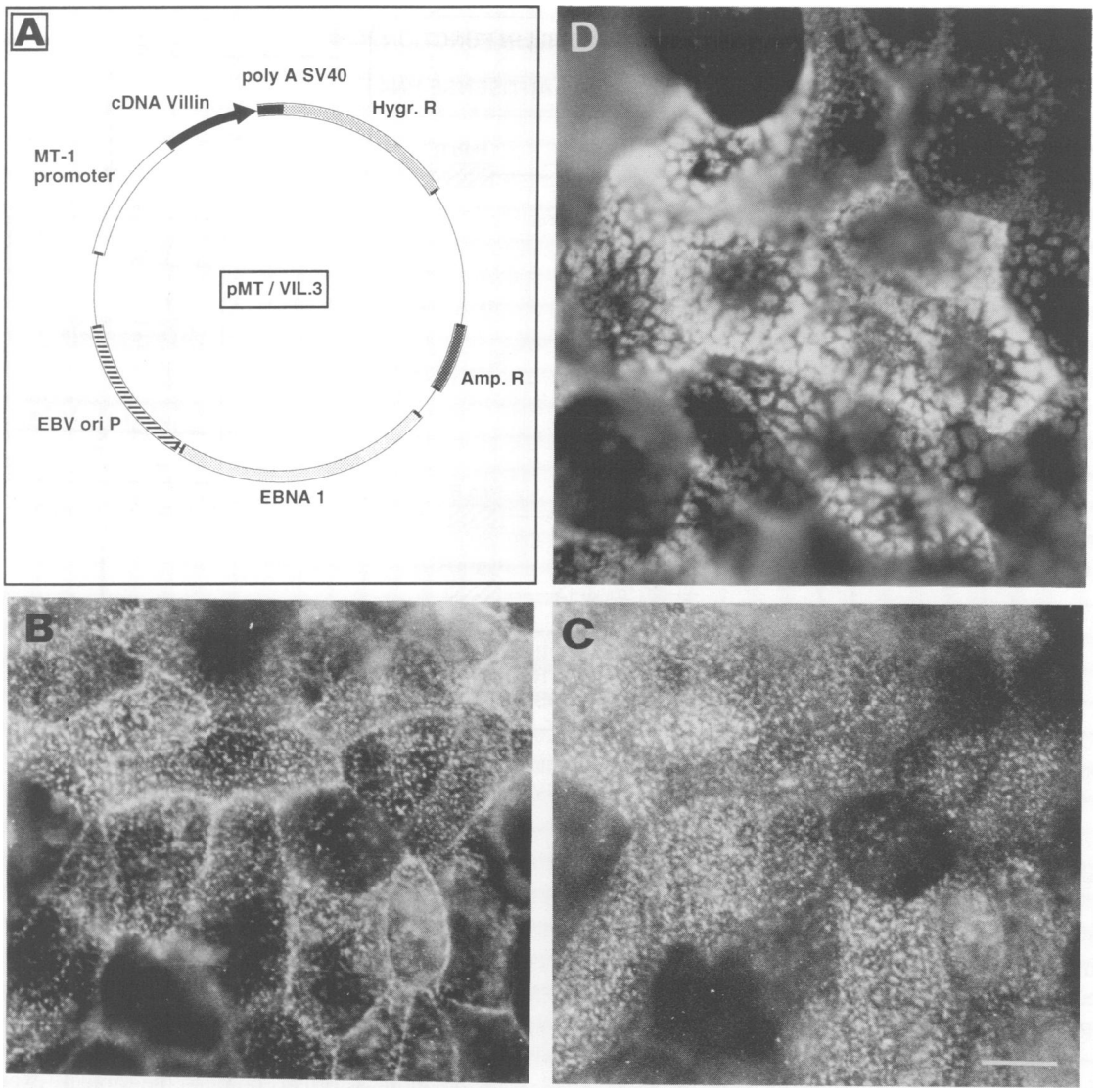

Fig. 8. Titration of antisense villin RNA in CaCO2 AS 4.8/34 cells with a partial sense villin RNA restores the parental CaCO2 phenotype. **(A)** Structure of the human villin sense expression vector, pMT/VIL3. A 925 bp *BglII* fragment of the human villin cDNA was inserted in the sense orientation into the eukaryotic episomal vector pMT/EP. Transcription of the sense cDNA fragment is driven by the MT-I promoter. The SV40 poly(A) provides the RNA processing signal. The $Hygr^R$ confers resistance to hygromycin B. The origin of replication (EBV ori-P) and the EBV-encoded nuclear antigen I allow pMT/VIL3 to replicate as an episome in human eukaryotic cells. **(B–D)** CaCO2 AS 4.8/34 cells were transfected with the partial villin sense cDNA inserted into the pMT/EP vector. The hygromycin-resistant clones were pooled and referred to as CaCO2/34/pMT. Immunolabeling with antibodies for F-actin, villin and SI was performed 14 days after confluency as described previously. (B and C) Double labeling of permeabilized CaCO2/34/pMT cells with rhodamine-coupled phalloidin (B) and a polyclonal anti-villin antibody (C). Villin is once again expressed at the apical surfaces of large islands of CaCO2/34/pMT cells, and colocalizes with the F-actin labeling. (D) Immunolocalization of SI in non-permeabilized CaCO2/34/pMTVIL3 cells using a polyclonal anti-SI antibody. Apical expression of SI is restored in the double-transfected cells. The pattern and intensity of the staining are nearly identical to that observed in untransfected cells (see Figure 7c for comparison). Bar corresponds to 10 μm.

human intestinal CaCO2 cell line. Permanent inhibition of villin synthesis, achieved by the overexpression of villin antisense RNA in stable CaCO2 subclones, markedly impairs brush-border assembly. We conclude, therefore, that villin function is not redundant and that no alternative pathway for brush-border assembly seems to exist (at least in CaCO2 cells), or is able to compensate for the absence of villin. Thus, villin is an early initiator of microvillar assembly and is part of an obligatory pathway for brush-border morphogenesis.

We trust that the experiments reported here and in an earlier study (Friederich *et al.*, 1989) provide a rational strategy for analyzing structure–function relationships of villin both at the cellular level and in the context of the whole organism. Experiments are underway in our laboratory which aim to knock out the unique villin gene in mice. This should enable us to confirm the extent to which *in vivo* brush-border assembly strictly requires villin. The CaCO2 AS 4.8/34 cell line should enable us to dissect at the cellular level the physiological disorders that we may discover in the organs of transgenic animals lacking the villin gene.

Correct assembly of a brush border is not required for cell polarity

CaCO2 AS 4.8/34 cells grown in monolayers were shown to exhibit the usual features of polarized epithelial cells. For instance, the junctional complexes appear unperturbed,

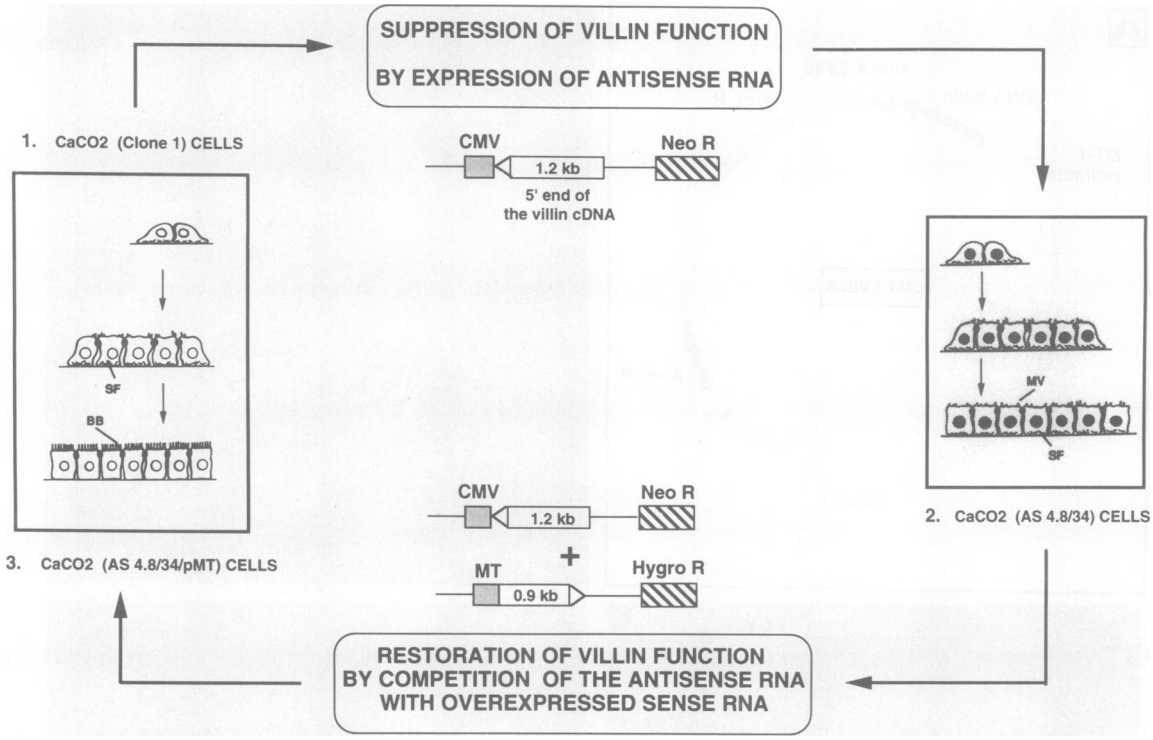

Fig. 9. Schematic diagram for the sustained suppression of villin in intestinal culture cells by an antisense RNA strategy followed by the restoration of the parental phenotype through the titration of these antisense RNA. MV, microvilli; BB, brush border; SF, stress fibers.

as verified by ultrastructural analysis and localization of the tight junction protein ZO1. Moreover, the distribution of some membrane protein markers for basolateral or apical surfaces is identical to that in the parental CaCO2 cell line. These results suggest two important points: (i) the proper localization of the tight junction is not affected by the diminution of the brush border, and (ii) these tight junctions are functional as they provide an efficient barrier for preventing the lateral diffusion of membrane proteins (DPP IV, nAP, nEP and gp120). In contrast, the organization of the cortical microfilament network in this subclone is significantly altered. For instance, stress fibers at the basal poles of confluent cells are normally few and poorly organized in the CaCO2 cells, but are numerous and well organized in CaCO2 AS 4.8/21 and CaCO2 AS 4.8/34 clones expressing low levels of villin. Conversely, densely packed microvilli containing F-actin are prominent at the cell apex of parental cells, but are scarce in the antisense villin-expressing cell lines. These observations, summarized in Figure 9, are reminiscent of those reported by Friederich *et al.* (1989) where it was shown that fibroblasts overexpressing villin displayed numerous dorsal microvilli but almost no actin stress fibers associated with their ventral faces. Thus, the presence or absence of a high level of villin correlates with the relative abundance of stress fibers, even in cells of different origins (fibroblasts, polarized epithelial cells). These data provide further evidence that villin is an efficient modulator of cortical actin microfilament organization.

We have therefore generated intestinal cells where the polarized distribution of plasma membrane protein markers is largely preserved, despite the fact that the distribution of specific cytoskeleton structures usually associated with distinct plasma membrane domains is altered.

Improper assembly of a brush border affects the cell-surface expression of an apical membrane protein, SI

In our hypomorphic CaCO2 AS 4.8/34 cells, which fail to develop a brush border, the apical expression of intestinal brush-border membrane protein SI is impaired and the hydrolase accumulates in intracellular structures. In contrast, other apical hydrolases, such as DPP IV, nAP and nEP, were shown to be correctly localized. While we cannot distinguish whether an organized brush border is necessary for the insertion or stabilization of SI at the apical membrane, we can conclude that the apical steady-state distribution of SI requires a morphologically distinct brush border. These results provide further evidence that the CaCO2 cell line makes use of at least two distinct pathways for the transport of apical membrane proteins. It is known that DPP IV and nAP are membrane proteins which are first inserted into the basolateral membrane, and then subsequently retrieved by transcytosis to the apical surface (Le Bivic *et al.*, 1990; Matter *et al.*, 1990). In contrast, SI and several GPI-linked proteins, such as carcino-embryonic antigen (CEA) and alkaline-phosphatase, are directly transported from the trans-Golgi network (TGN) to the apical surface (Lisanti and Rodriguez-Boulan, 1990).

While cytoskeleton−membrane protein interactions are poorly understood at the level of the brush border, such interactions have been described in other systems (Bretscher, 1991; Luna and Hitt, 1992) and often follow the paradigm originally described for the human red blood

cell (Branton *et al.*, 1981; Goodman *et al.*, 1988; Bennett, 1989, Palek and Sahr, 1992). In addition to regulating cell and membrane shape, the interactions between cytoskeleton and plasma membrane also serve to stabilize cell−cell or cell−substrate attachments (Luna and Hitt, 1992), and to generate epithelial membrane polarity. For example, transfection of the epithelial cell adhesion molecule (L-CAM or uvomorulin) into fibroblasts was believed to be sufficient to induce a 'lateral' distribution of fodrin and Na^+,K^+-ATPase to areas of uvomorulin-mediated cell−cell contacts (McNeill *et al.*, 1990). In the context of the aforementioned studies, it seems likely that the actin cytoskeleton of brush-border microvilli may be involved in both the morphogenesis of the brush border and the retention and/or targeting of its resident specific membrane proteins such as SI. We are presently exploring the extent to which SI apical expression requires a highly differentiated membrane scaffold to mediate the proper interactions between transport vesicles, plasma membrane components and the cortical actin cytoskeleton.

Phenotype rescue by super-transfection of a sense RNA encoding plasmid

Since we have shown previously that a transfected Neo^R CaCO2 cell line (CaCO2 pPrVL) presents a polarized phenotype comparable with parental CaCO2 cells (Robine *et al.*, 1993), it is unlikely that the CaCO2 AS 4.8/21 and CaCO2 AS 4.8/34 phenotypes are a consequence of clonal selection. It is also unlikely that the observed phenotype is due to the disruption of a host cell gene required for brush-border assembly. First, we have obtained two independent clones in which the phenotype correlates directly with the residual level of villin expressed. Second, abortive brush-border assembly can be fully reversed by titrating the villin antisense RNA with complementary partial sense RNA. Such an approach has been reported previously to reverse the effect of protein 4.1 antisense RNA microinjection into *Xenopus* embryos (Giebelhaus *et al.*, 1988) which disturb the retinal cellular interactions during embryonic development. This phenotype could be rescued by the microinjection of plasmid that expressed partial-length sense protein 4.1 RNA. To our knowledge, titration of antisense RNA in a stable cell line through the super-transfection of a sense RNA-encoding construct has never been reported before. Using this experimental approach we were able to show that the re-expression of villin restores both the structural and functional properties (i.e. SI apical expression) of a brush-border domain.

Conclusion

A schematic representation of our CaCO2 AS 4.8/34 cell model is summarized in Figure 9. Our antisense expression strategy has allowed us to generate a cell culture system of hypomorphic intestinal cells which will be suitable for further studies into the structure−function relationships of a well-developed brush border. Furthermore, this cellular model might also facilitate the study of certain *in vivo* disease states, such as microvillar atrophy (Phillips *et al.*, 1985) and congenital SI deficiency (Hauri *et al.*, 1985a; Lloyd and Olsen, 1987; Naim *et al.*, 1988).

Materials and methods

Plasmids

The plasmid pSVNeo (kindly provided by J.P.Rousset, Pasteur Institute, Paris, France) includes the neomycin resistance gene (Neo^R) under the control of the SV40 early promoter. The plasmid pCB6 (kindly provided by D.Russel, University of Texas, Southwestern Medical Center, Dallas, TX) includes the CMV promoter, a multiple cloning site, the human growth hormone (hGH) terminator and Neo^R as a selectable marker. The plasmid pMT/EP (Trojan *et al.*, 1992; kindly provided by J.Ilan, Case Western Reserve University, Cleveland, OH) includes the mouse MT-I promoter which is inducible with heavy metals (Stuart *et al.*, 1984), a multiple cloning site, the SV40 poly(A) signal, an Epstein−Barr virus (EBV) origin of replication (ori-P) and the EBV-encoded nuclear antigen I which allow an episomal replication in human eukaryotic cells (Yates *et al.*, 1985). This vector contains the hygromycin resistance gene (Hyg^R) as a selectable marker.

Construction of vectors expressing partial sense and antisense villin RNA

Standard procedures, as described by Sambrook *et al.* (1989), were used for DNA engineering. A 1274 bp *Kpn*I fragment from the full-length human villin cDNA (Arpin *et al.*, 1988), comprising 40 bp of the 5′ non-coding region, the ATG translation initiation codon and 1231 bp of the coding sequence, was inserted at the *Kpn*I site of the pCB6 plasmid. An antisense clone with reference to the CMV promoter was identified by restriction and DNA sequencing analysis, and was referred to as pCB6 AS 4.8. A 925 bp *Bgl*II fragment from the full-length human villin cDNA, comprising 40 bp of the 5′ non-coding region, the ATG translation initiation codon and 882 bp of the coding sequence, was inserted at the *Bam*HI site of the pMT/EP plasmid. A sense clone with reference to the MT-I promoter was identified by restriction analysis and referred to as pMT/VIL3.

Cell culture

CaCO2 clone 1 cells were isolated from the parental human CaCO2 cell line (Fogh and Trempe, 1975) by two rounds of limiting dilution and glass cylinder cloning, followed by selection based on homogeneity and a high degree of terminal differentiation. This CaCO2 subclone was grown in Dulbecco's minimum essential medium (DMEM) supplemented with 10% fetal calf serum at 37°C under a 10% CO_2 atmosphere, as described for the parental CaCO2 cell line (Pinto *et al.*, 1983). The fibroblast-like CV1 cells (Jensen *et al.*, 1964) were grown under the same conditions.

Transfections

CaCO2 clone 1 cells were transfected with the plasmid pCB6 AS 4.8 using lipofectin reagent (Gibco/BRL) according to the supplier's instructions (Felgner *et al.*, 1987). After transfection, cells were grown until they reached 80% confluency and then were replated at low density. The selection of stable transfectants was accomplished by the addition of 0.7 mg/ml G418 (Gibco/BRL) to the culture medium. In all, 50 cell colonies resistant to G418 were isolated using cloning rings and were amplified separately. About 50% of these colonies did not grow after glass cylinder isolation. The remaining cell clones were screened for villin expression by Western blot analysis (see below). Two of them, CaCO2 AS 4.8/21 and CaCO2 AS 4.8/34, were analyzed in detail. The CaCO2 AS 4.8/34 cell clone was then super-transfected with the plasmid pMT/VIL3 using the same procedure. The selection of stable transfectants was accomplished by the addition of 200 U/ml hygromycin B (Calbiochem) to the culture medium. Cell colonies resistant to hygromycin B were pooled and referred to as CaCO2/34/pMT.

CV1 cells were transfected with the plasmid pCB6 AS 4.8 as described for CaCO2 clone 1 cells. Two days after transfection, cells were collected to prepare total RNA extracts.

A pPrVL CaCO2 subclone was generated in our laboratory by stable cotransfection of the parental CaCO2 clone 1 cells with the pSVneo and the pPrVL plasmids using the same procedure as that described above (Robine *et al.*, 1993). The pSVneo plasmid contains Neo^R under the control of the viral SV promoter. The pPrVL plasmid contains a genomic fragment corresponding to 2 kb of 5′ flanking region of the human villin gene, upstream of the firefly luciferase gene (as a neutral gene). We used this subclone to show that transfection and cell cloning procedures gave rise to a fully differentiated CaCO2 subclone, as confirmed by dome formation after cell confluency, a high level of villin expression and the apical localization of SI.

DNA amplification (PCR)

Amplification of fragments from the villin cDNA was performed with the Perkin-Elmer/Cetus thermal cycler using cloned *Taq* polymerase (Cetus). The amplification protocol employed 35 cycles at 92°C for 1 min, 55°C for 1 min and 72°C for 3 min, with an increase of 2 s per cycle for the 72°C step. Oligonucleotides (Genset) were selected to discriminate amplified products of the transfected cDNA from the endogenous villin gene. The coding primer (CTGACTCCGAGGGG-AATCTG) was positioned in the seventh exon (encompassing +800 to +819 on the villin cDNA) and the non-coding primer (GCTTTCTTCCC-TTTCCACAC) in the eighth exon (encompassing +913 to +932 on the villin cDNA). On the endogenous gene, the intron (no. 7) between these two exons encompasses 150 bp (Pringault *et al.*, 1991). Thus, the predicted sizes of the amplified fragments from the transfected cDNA and endogenous gene were 133 and 283 bp, respectively.

RNA analysis

Total cellular RNA was prepared by the method of Chomczynski and Sacchi (1987).

Uniformly radiolabeled RNA probes were synthesized with T3 and T7 RNA polymerases using plasmid M84 as matrix. The plasmid M84 was generated by the insertion of a 250 bp fragment of the villin cDNA spanning from +290 to +540, into the Blue-Scribe vector. After linearization with *Eco*RI, transcription with T3 RNA polymerase generated an antisense 260 nucleotide probe; after linearization with *Hin*dIII, transcription with T7 RNA polymerase generated a sense 257 nucleotide probe.

Northern blot experiments were performed as described previously (Arpin *et al.*, 1988).

Standard procedures, as described by Sambrook *et al.* (1989), were used for RNase protection assays. Hybridization was performed with 5 μg of RNA and 2.5×10^5 c.p.m. of labeled RNA probe (1×10^8 c.p.m./μg). Unhybridized material was removed by digestion with RNase A (40 μg/ml) and RNase T1 (2 μg/ml). After inactivation of the RNase and precipitation, the samples were loaded onto 8% denaturing polyacrylamide gels (Maxam and Gilbert, 1980). Gels were exposed to film at −80°C for 3 days.

Antibodies

For immunodetection of villin, we used a polyclonal anti-villin antibody (serum 1.135) or a monoclonal anti-villin antibody (ID2C3; Dudouet *et al.*, 1987). Polyclonal anti-nEP antibody was kindly provided by P.Crine, Université de Montreal, Canada; polyclonal anti-nAP antibody (3.01.01.75) was kindly provided by S.Maroux, Marseille, France; monoclonal anti-DPP IV antibody (Hauri *et al.*, 1985b) and anti-120 kDa basolateral membrane glycoprotein (BIMg) antibody (Eilers *et al.*, 1989) were kindly provided by H.P.Hauri, Université de Bâle, Switzerland; polyclonal anti-ZO1 tight junction protein antibody (Anderson *et al.*, 1989) was kindly provided by J.Anderson, Yale University, New Haven, CT; affinity-purified polyclonal anti-actin antibody was kindly provided by G.Gabbiani, Université de Genève, Switzerland; polyclonal anti-SI antibody was kindly provided by I.Chantret, INSERM U 178, Villejuif, France. Alkaline phosphatase-conjugated anti-IgG antibodies (Promega) were used for Western blot analysis. Fluorescein and rhodamine-conjugated anti-IgG antibodies (Amersham) were used for immunocytochemistry.

Western blot analysis

A total of 100 μg of total protein from post-confluent cells were isolated using the procedure of Burnette (1981), as modified by Coudrier *et al.* (1983). Proteins were fractionated by SDS−PAGE analysis and then subjected to Western analysis using villin and actin-specific primary antibodies, followed by alkaline phosphatase-conjugated secondary antibody.

Immunocytochemistry

Markers for epithelial polarity were localized on cells grown on glass coverslips 15–21 days after confluency (villin, DPP IV, SI, ZO1 and gp120). Immunocytochemical procedures have been described in detail by Reggio *et al.* (1983). Briefly, confluent cells were fixed with 3% paraformaldehyde and permeabilized (where indicated) with 2% Triton X-100 in PBS. Cells were incubated with the primary antibody at the appropriate dilution in a humidified atmosphere. After washing, cells were then incubated with 10 μg/ml fluorescein or rhodamine-conjugated anti-IgG secondary antibodies. For F-actin labeling, cells were incubated with 0.3 μg/ml rhodamine-conjugated phalloidin. All preparations were examined under a Zeiss photomicroscope equipped for epifluorescence optics or by CLSM. The cell monolayer was optically sectioned in horizontal ($x-y$) or vertical planes ($x-z$) every 0.8 μm. Nuclei were visualized by incubating cells with 2 μg/ml propidium iodine (during the first wash following the incubation with secondary antibody). Recorded images were photographed from the screen using a freeze-frame Polaroid system.

Electron microscopy

Cells grown to confluency on plastic supports were rinsed in PBS, fixed for 2 h with 2.5% glutaraldehyde in PBS, post-fixed in 1% osmium, dehydrated in a graded series of ethanol dilutions and embedded in Epoxy resin. Ultrathin sections were cut from transversely orientated confluent monolayers, counterstained with uranyl acetate and lead citrate, and examined under a Philips electron microscope (EM 410). Cell preparations for scanning electron microscopy were fixed, dehydrated in a series of ethanol washes, as described previously, and then placed in Freon 113 and dried after substitution with liquid CO_2 in a critical point dryer (Balzers, Hudson, NH). Specimens were coated with gold and examined with a Jeol 35CS scanning electron microscope.

Acknowledgements

We thank Dr C.Gottardi for critically reading the manuscript and for helpful comments. We wish to thank M.Lesourd and P.Gounon for their technical assistance in scanning electron microscopy and J.C.Benichou for his technical assistance in transmission electron microscopy. We thank Dr Ch.Huet for his helpful suggestions in morphological analysis. Thanks are also due to R.Hellio for his help in confocal laser scanning microscopy and to R.Carré for her diligent help in the preparation of this manuscript. We are grateful to E.Caliot for her help in cell culture. We thank N.Bouvier for his skills in producing the art drawings. This work was supported by grants from the Association pour la Recherche sur le Cancer (ARC no. 6379), the Fondation pour la Recherche Médicale and the Institut National de la Santé et de la Recherche Médicale (INSERM no. 920204). M.A.C.B. is a recipient of fellowships from the Fondation pour la Recherche Médicale and the Ligue Nationale Française contre le Cancer.

References

Anderson,J.M., Van-Itallie,C.M., Peterson,M.D., Stevenson,B.R., Carew, E.A. and Mooseker,M.S. (1989) *J. Cell Biol.*, **109**, 1047–1056.

Arpin,M. and Friederich,E. (1992) In Fleming,T.P. (ed.), *Epithelial Organization and Development.* Chapman and Hall, London, UK, pp. 245–271.

Arpin,M., Pringault,E., Finidori,J., Garcia,A., Jeltsch,J.-M., Vandekerckhove,J. and Louvard,D. (1988) *J. Cell Biol.*, **107**, 1759–1766.

Bennett,V. (1989) *Biochim. Biophys. Acta*, **988**, 107–121.

Boller,K., Arpin,M., Pringault,E. and Reggio,H. (1988) *Differentiation*, **39**, 51–57.

Branton,D., Cohen,C.M. and Tyler,J. (1981) *Cell*, **24**, 24–32.

Bretscher,A. (1991) *Annu. Rev. Cell Biol.*, **7**, 337–374.

Burnette,W.N. (1981) *Anal. Biochem.*, **112**, 195–203.

Chomczynski,P. and Sacchi,N. (1987) *Anal. Biochem.*, **162**, 156–159.

Colman,A. (1990) *J. Cell Sci.*, **97**, 399–409.

Coluccio,L.M. and Bretscher,A. (1989) *J. Cell Biol.*, **108**, 495–502.

Coudrier,E., Reggio,H. and Louvard,D. (1983) *EMBO J.*, **2**, 469–475.

Dudouet,B., Robine,S., Huet,C., Sahuquillo-Merino,C., Blair,L., Coudrier,E. and Louvard,D. (1987) *J. Cell Biol.*, **105**, 359–369.

Eilers,U., Klumperman,J. and Hauri,H.P. (1989) *J. Cell Biol.*, **108**, 13–22.

Ezzel,R.M., Chafel,M.M. and Matsudaira,P.T. (1989) *Development*, **106**, 407–419.

Felgner,P.L., Gadeck,T.R., Holm,M., Roman,R., Chan,H.W., Wenz,M., Northrop,J.P., Ringold,J.M. and Danielsen,M. (1987) *Proc. Natl Acad. Sci. USA*, **84**, 7413–7417.

Fogh,J. and Trempe,G. (1975) In Fogh,J. (ed.), *Human Tumor Cells in Vitro.* Plenum Publishing Corp., New York, pp. 115–141.

Friederich,E., Huet,C., Arpin,M. and Louvard,D. (1989) *Cell*, **59**, 461–475.

Friederich,E., Vancompernolle,K., Huet,C., Goethals,M., Finidori,J., Vandekerckhove,J. and Louvard,D. (1992) *Cell*, **70**, 81–92.

Giebelhaus,D.H., Eib,D.W. and Moon,R.T. (1988) *Cell*, **53**, 601–615.

Goodman,S.R., Krebs,K.E., Whitfield,C.F., Riederer,B.M. and Zagon,I.S. (1988) *CRC Crit. Rev. Biochem.*, **23**, 171–234.

Hauri,H.P., Roth,J., Sterchi,E.E. and Lentze,M. (1985a) *Proc. Natl Acad. Sci. USA*, **82**, 4423–4427.

Hauri,H.P., Sterchi,E.E., Bienz,D., Fransen,J.A.M. and Marxer,A. (1985b) *J. Cell Biol.*, **101**, 838–851.
Heintzelman,M.B. and Mooseker,M.S. (1992) *Curr. Top. Dev. Biol.*, **26**, 93–122.
Izant,J.G. and Weintraub,H. (1985) *Science*, **229**, 345–352.
Jensen,F.C., Girardi,A.J., Gilden,R.V. and Koprowski,H. (1964) *Proc. Natl Acad. Sci. USA*, **52**, 53–64.
Katsuki,M., Sato,M., Kimura,M., Yokoyama,M., Kobayashi,K. and Nomura,T. (1988) *Science*, **241**, 593–595.
Kim,S. and Wold,B. (1985) *Cell*, **42**, 129–138.
Knecht,D.A. and Loomis,W.F. (1987) *Science*, **236**, 1081–1086.
Landry,C., Huet,C., Mangeat,P., Sahuquet,A., Louvard,D. and Crine,P. (1994) *Differentiation*, **56**, 55–65.
Le Bivic,A., Quaroni,A., Nichols,B. and Rodriguez-Boulan,H. (1990) *J. Cell Biol.*, **111**, 1351–1361.
Lisanti,M.P. and Rodriguez-Boulan,H. (1990) *Trends Biochem. Sci.*, **15**, 113–118.
Lloyd,M.L. and Olsen,W.A. (1987) *N. Engl. J. Med.*, **316**, 438–442.
Louvard,D. (1980) *Proc. Natl Acad. Sci. USA*, **77**, 4132–4136.
Luna,J.L. and Hitt,A.L. (1992) *Science*, **258**, 955–964.
Mamajiwalla,S.N., Fath,K.R. and Burgess,D.R. (1992) *Curr. Top. Dev. Biol.*, **26**, 123–143.
Matter,K., Brauchbar,M., Bucher,K. and Hauri,H.P. (1990) *Cell*, **60**, 429–437.
Maxam,A. and Gilbert,W. (1980) *Methods Enzymol.*, **65**, 499–560.
McNeill,H., Ozawa,M., Kemler,R. and Nelson,W.J. (1990) *Cell*, **62**, 309–316.
Naim,H.Y., Roth,J., Sterchi,E.E., Lentze,M., Milla,P., Schmitz,J. and Hauri,H.P. (1988) *J. Clin. Invest.*, **82**, 667–679.
Palek,J. and Sahr,K.E. (1992) *Blood*, **80**, 308–330.
Peterson,M. and Mooseker,M. (1992) *J. Cell Sci.*, **102**, 581–600.
Peterson,M.D. and Mooseker,M.S. (1993) *J. Cell Sci.*, **105**, 445–460.
Peterson,M.D., Bement,W.M. and Mooseker,M.S. (1993) *J. Cell Sci.*, **105**, 461–472.
Phillips,A.D., Jenkins,P., Raafat,F. and Walker-Smith,J.A. (1985) *Arch. Dis. Child.*, **60**, 135–140.
Pinto,M. *et al.* (1983) *Biol. Cell.*, **47**, 323–330.
Pollenz,R.S., Chen,T.L.L., Trivinos-Lagos,L. and Chisholm,R.L. (1992) *Cell*, **69**, 951–962.
Pringault,E., Arpin,M., Garcia,A., Finidori,J. and Louvard,D. (1986) *EMBO J.*, **5**, 3119–3124.
Pringault,E., Robine,S. and Louvard,D. (1991) *Proc. Natl Acad. Sci. USA*, **88**, 10811–10815.
Reggio,H., Webster,P. and Louvard,D. (1983) *Methods Enzymol.*, **98**, 379–396.
Robine,S., Huet,C., Moll,R., Sahuquiłlo-Merino,C., Coudrier,E., Zweibaum,A. and Louvard,D. (1985) *Proc. Natl Acad. Sci. USA*, **82**, 8488–8492.
Robine,S., Sahuquillo-Merino,C., Louvard,D. and Pringault,E. (1993) *J. Biol. Chem.*, **268**, 11426–11434.
Rodriguez Fernandez,J.L., Geiger,B., Salomon,D. and Ben-Ze'ev,A. (1993) *J. Cell Biol.*, **122**, 1285–1294.
Sambrook,J., Fritsch,E.F. and Maniatis,T. (1989) *Molecular Cloning: A Laboratory Manual.* 2nd edn. Cold Spring Harbor Laboratory Press, Cold Spring Harbor, NY.
Shibayama,T., Carboni,J.M. and Mooseker,M.S. (1987) *J. Cell Biol.*, **105**, 335–344.
Stuart,G.W., Searle,P.F., Chen,H.Y., Brinster,R.L. and Palmiter,R.D. (1984) *Proc. Natl Acad. Sci. USA*, **81**, 7318–7322.
Trojan,J., Blossey,B.K., Johnson,T.R., Rudin,S.D., Tykocinski,M. and Ilan,J. (1992) *Proc. Natl Acad. Sci. USA*, **89**, 4874–4878.
Weinstein,D.E., Michael,L.S. and Liem,R.K.H. (1991) *J. Cell Biol.*, **112**, 1205–1213.
Yates,J.L., Warren,N. and Sugden,B. (1985) *Nature*, **313**, 812–815.

Received on September 12, 1994; revised on November 21, 1994